



# 3'UTR RNA editing driven by ADAR1 modulates MDM2 expression in breast cancer cells

Elanur Almeric<sup>1</sup> · Deniz Karagozolu<sup>1</sup> · Mustafa Cicek<sup>1,2</sup> · Didem Naz Dioken<sup>1</sup> · Huseyin Avni Tac<sup>3</sup> ·  
Esra Cicek<sup>1</sup> · Busra Aytul Kirim<sup>4</sup> · Irmak Gurcuoglu<sup>1</sup> · Osman Ugur Sezerman<sup>3</sup> · Nurhan Ozlu<sup>4</sup> ·  
Ayse Elif Erson-Bensan<sup>1,5</sup>

Received: 25 February 2025 / Revised: 29 April 2025 / Accepted: 2 May 2025  
© The Author(s) 2025

## Abstract

Epitranscriptomic changes in the transcripts of cancer related genes could modulate protein levels. RNA editing, particularly A-to-I(G) editing catalyzed by ADAR1, has been implicated in cancer progression. RNA editing events in the 3' untranslated region (3'UTR) can regulate mRNA stability, localization, and translation, underscoring the importance of exploring their impact in cancer. Here, we performed an in silico analysis to detect breast cancer enriched RNA editing sites using the TCGA breast cancer RNA-seq dataset. Notably, the majority of differential editing events mapped to 3' untranslated regions (3'UTRs). We confirmed A-to-I(G) editing in the 3'UTRs of *MDM2* (Mouse Double Minute 2 homolog), *GINS1* (GINS Complex Subunit 1), and *F11R* (Junctional Adhesion Molecule A) in breast cancer cells. RNA immunoprecipitation with ADAR1 antibody confirmed the interaction between ADAR1 and *MDM2*, *GINS1*, and *F11R* 3'UTRs. ADAR1 knockdown revealed decreased editing levels, establishing ADAR1 as the editing enzyme. A reporter assay for *MDM2*, an oncogene overexpressed mostly in luminal breast cancers, demonstrated that RNA editing enhances protein expression, in agreement with reduced MDM2 protein levels in ADAR1 knockdown cells. Further exploration into the mechanisms of 3'UTR editing events revealed an interaction between ADAR1 and CSTF2, a core component of the polyadenylation machinery, as identified through biotin-based proximity labeling mass spectroscopy, and co-immunoprecipitation experiments. Furthermore, CSTF2 knockdown reduced both ADAR1 and MDM2 protein levels. Our findings highlight implications for *MDM2* regulation by ADAR1-dependent 3'UTR RNA editing and present an interplay between RNA editing on 3'UTRs and the mRNA polyadenylation machinery. These results improve our understanding of ADAR1's role in cancer-associated 3' UTR RNA editing and its potential as a therapeutic target.

**Keywords** RNA editing · 3'UTR · MDM2 · GINS1 · F11R · ADAR1 · CSTF2 · Proximity biotinylation

## Introduction

The mammalian transcriptome is highly diversified through various mechanisms, including RNA modifications. RNA editing by ADAR enzymes is one of the most prominent examples of widespread RNA modifications. RNA editing involves the deamination of adenosine to inosine or cytosine to uracil. Adenosine-to-inosine (A-to-I) RNA editing is catalyzed by adenosine deaminases (i.e., ADARs), subsequently leading inosines to be recognized as guanosines due to their similar electrostatic potential (Bass 2002). As a result, A-to-I editing within coding regions can modify codons, resulting in the production of altered protein isoforms (Maas et al., 2006). In untranslated regions (UTRs), RNA editing can influence RNA stability, localization,

✉ Ayse Elif Erson-Bensan  
erson@metu.edu.tr

<sup>1</sup> Department of Biological Sciences, Middle East Technical University (METU), Dumlupinar Blvd. No.1 Universiteler Mah, Cankaya, Ankara 06800, Türkiye

<sup>2</sup> Department of Biology, Kamil Ozdag Faculty of Science, Karamanoglu Mehmetbey University, Karaman, Türkiye

<sup>3</sup> School of Medicine, Department of Basic Sciences, Biostatistics and Medical Informatics, Acibadem Mehmet Ali Aydinlar University, Istanbul, Türkiye

<sup>4</sup> Department of Molecular Biology and Genetics, Koc University, Rumelifeneri Yolu, Sariyer, Istanbul 34450, Türkiye

<sup>5</sup> Cancer Systems Biology Laboratory, CanSyL, METU, Ankara, Türkiye

translation and modulate interactions with trans-factors (Mendoza et al., 2024).

ADAR1 (ADAR) is widely expressed across the different organs of the body as the principal A-to-I RNA editor and exists in two isoforms: the interferon-inducible p150 and the constitutively expressed p110. ADAR1 mediates editing by binding to double-stranded RNA (dsRNA) regions, which are commonly formed by inverted repeats, such as *Alu* elements. However, secondary structures within non-repetitive sequences can also serve as editing substrates (Liu et al. 2024). ADAR2 (ADARB1) is predominantly expressed in the brain, editing transcripts expressed in the central nervous system. ADAR3 (ADARB2) is a brain-specific but catalytically inactive enzyme (Rehwinkel and Mehdipour 2025).

Deregulated RNA editing has been implicated in various diseases, including neurodevelopmental disorders, autoimmune conditions, and cancer (Bass 2002). Notably, advancements in RNA sequencing technologies have brought increasing attention to the widespread nature and role of A-to-I(G) modifications in cancer. Numerous studies have shown that both ADAR1 levels and editing levels are markedly altered in many malignant tumors, with strong correlations to tumor progression and proteomic diversity in cancer (Zhang et al. 2024; Peng et al. 2018). However, the role of RNA editing in the non-coding regions of cancer-related genes remains to be further investigated.

In this study, we investigated ADAR1-mediated A-to-I(G) RNA editing events in breast cancer, with a focus on 3'UTRs. Using TCGA RNA-seq data, we identified differentially edited 3'UTRs in breast cancers and experimentally validated editing sites in the 3'UTRs of *MDM2*, *GINS1*, and *F11R* regulated by ADAR1 with protein level implications. We also provide insight into ADAR1 interaction with the polyadenylation machinery, supporting the possibility that ADAR1 may associate with transcripts at or near their 3'UTRs. These findings underscore ADAR1's regulatory role in cancer and its potential as a therapeutic target.

## Methods

### In silico analysis

RNA editing regions in tumor ( $n=837$ ) and normal samples ( $n=105$ ) of the TCGA Breast Cancer RNA-seq were taken from the Synapse database (SynID: syn2374375) (<https://www.synapse.org/>) (Han et al. 2015). RNA editing sites which were present in at least 5 pairs of tumor and non-tumor samples were selected as informative RNA editing sites. Wilcoxon test was used to detect differential editing between tumor and non-tumor samples. Significantly

different editing sites were defined with  $FDR < 0.05$  and a mean editing level difference  $\geq 5\%$  between tumor and non-tumor samples. RNA editing sites were annotated using R package "Annotatr" with human genome assembly GRCh37 (hg19) and were matched to corresponding gene IDs. An UpSet plot was generated using the Python upsetplot package to visualize the intersection of editing regions on single mRNAs to identify patterns of possible co-occurrence.

### Cell lines and growth conditions

MCF7, T47D and MDA-MB-231 breast cancer cells and cells were cultured in Dulbecco's Modified Eagle Medium (DMEM) supplemented with 10% Fetal Bovine Serum (FBS) (Biowest, S1810-500), 2% L-Glutamine, 1% Sodium Pyruvate Solution and 1% Penicillin/Streptomycin (BI, 03-031-1B). Cells were incubated at 37 °C with 95% humidified air and 5% CO<sub>2</sub> and were grown as monolayers. Normal breast tissue cDNA was used from Breast Cancer cDNA Array IV (Origene).

### DNA, RNA isolation and RT-PCR

Genomic DNA (gDNA) was isolated from cell pellets using the lysis buffer (Tris-HCl (pH 8.5), EDTA, NaCl, and SDS). Following proteinase K and RNase A treatments, DNA was precipitated with ethanol and sodium acetate. Total RNA was extracted using the High Pure RNA Isolation Kit (Roche, 11828665001). RNA samples were DNase-treated (Thermo Fisher Scientific, EN0521) to eliminate DNA contamination. DNA and RNA quantity and purity were assessed using a MaestroNano spectrophotometer. cDNA was synthesized using the RevertAid First Strand cDNA Synthesis Kit (Thermo Fisher Scientific, K1622) using oligo(dT) primers. RT-PCR primers were designed from regions flanking the editing sites. PCR amplification was performed using Phusion™ High-Fidelity DNA Polymerase (Thermo Fisher Scientific, F530S). Following gel electrophoresis, PCR amplicons were extracted using Monarch® DNA Gel Extraction Kit (NEB, T1020) according to the manufacturer's protocol and sequenced using MiSeq NGS System (Illumina).

### Reporter assay

Edited and non-edited regions were designed as double-stranded oligos. Annealed oligos were cloned into pMIR-Report (pMIR). Cells were co-transfected with pMIR (*Firefly* luciferase) and phRL-TK (*Renilla* luciferase) using TurboFect (Thermo Fisher). Twenty-four hours after transfection, dual luciferase activities were measured using the Dual-Luciferase® Reporter Assay (Promega). Firefly/

Renilla ratios were normalized to that of the empty pMIR transfected cells.

### ADAR1 and CSTF2 silencing

FlexiTube GeneSolution for ADAR1 (QIAGEN, GeneGlobe Id: GS103, 1027416), CSTF2 FlexiTube GeneSolution for CSTF2 (QIAGEN, Gene Globe Id: GS1478, 1027416), and negative control siRNA (5 nmol) (QIAGEN, 1022076) were used. A 50 nM siRNA cocktail was prepared with 200  $\mu$ l of DMEM with 4500 mg/L high glucose and 4  $\mu$ l TurboFect Transfection Reagent (Thermo-Scientific/R0531).

### RNA immunoprecipitation

RNA Immunoprecipitation (RIP) protocol was performed as described (Peritz et al. 2006). Approximately,  $9 \times 10^6$  MCF7 cells were lysed in polysome lysis buffer. For RIP, ADAR1 antibody (Abcam, ab168809), or normal rabbit IgG control (Cell Signaling, 2729) and Protein A/G magnetic beads were used. Following RNA extraction with phenol-chloroform-isoamyl alcohol, RNA concentrations were determined. cDNA was synthesized using the ProtoScript<sup>®</sup> First Strand cDNA Synthesis Kit (NEB, E6300S) with d(T)23VN primers.

### CSTF2-TurboID plasmid

CSTF2 coding sequence (NM\_001325.2) was retrieved from NCBI and cloned into TurboID\_HA-pcDNA 3.1. TurboID vector was a kind gift from Prof. M. Muyan (METU). The cloned plasmid was confirmed by sequencing.

### Proximity-dependent biotinylation

CSTF2\_TurboID\_HA or just TurboID\_HA (empty vector) constructs were transfected into MCF7 cells. After 48 h, cells were transfected with CSTF2\_TurboID or TurboID control plasmid. 24 h later, CSTF2-TurboID transfected cells were either treated with 100 nM E2 (17 $\beta$ -Estradiol, Sigma 1250008) or ethanol. CSTF2\_TurboID\_HA-transfected cells were also treated with 50  $\mu$ M Biotin (D-Biotin, Sigma-Aldrich, B-4639), and 1 mM ATP (Sigma-Aldrich, adenosine 5'-triphosphate disodium salt hydrate, A2383) for 3 h. Nuclear and cytoplasmic lysates were isolated and used for western blot analysis to determine fusion protein expression and biotinylation status using anti-HA (Abcam, ab9110), anti-ADAR1 (Abcam, ab168809), anti-CSTF2 (Abcam, ab72297), and anti-Biotin (Abcam, ab53494), anti-HDAC (Santa Cruz, sc-81598) and anti-TUBA1A (Cell Signaling, 2144) primary and appropriate secondary antibodies.

### Mass spectrometry analysis of TurboID samples

To identify prey proteins, (nuclear and cytoplasmic) biotinylated proteins bound to Neutravidin High-Capacity Agarose beads (Thermo Fisher Scientific, 29204) were sent to Koc University Proteomics Facility (KUPAM) for Liquid Chromatography–Mass Spectrometry (LC-MS/MS) analysis. Nuclear and cytoplasmic fractions were separately analyzed. Proteins bound to the beads were digested with trypsin (Thermo Pierce MS Grade Trypsin Protease), and peptide purification was performed using C18 StageTips (Thermo Fisher Scientific). Peptide analysis was conducted with the Q-Exactive Orbitrap LC-MS/MS mass spectrometer (Thermo Fisher Scientific), and protein identification was carried out using the Proteome Discoverer 1.4 software (Thermo Fisher Scientific). Any cytoplasmic protein was removed the nuclear lysate list and was not included in further analysis. SAINT (Significance Analysis of INTERactome) was used as a statistical tool to estimate the probability of protein-protein interactions using default parameters, comparing E2 treated and control cell nuclear samples (Choi et al. 2011). Proteins with a SAINT score greater than 0.5 and a BFDR (Bayesian False Discovery Rate) lower than 0.05 were considered significant.

### Co-immunoprecipitation

Nuclear lysates were prepared from MCF7 cells using NEPER<sup>™</sup> Nuclear and Cytoplasmic Extraction Kit (Thermo Fisher Scientific). Protein A/G magnetic beads (New England BioLabs) were blocked overnight with BSA, washed, and incubated with primary antibodies (CSTF2, Santa Cruz sc-398862 or mouse IgG control, Santa Cruz sc-202) and protein lysates. Beads were washed, and bound proteins were eluted with SDS loading buffer and analyzed by immunoblotting using CSTF2 (Abcam, ab72297) and ADAR1 (Cell Signaling, 14175) antibodies. Blots were visualized using WesternBright ECL Blotting Substrates (Advantak12045-D50) on a ChemiDoc<sup>™</sup> MP Imaging System (BioRad, 170–8280).

### MDM2 mRNA and protein expression analysis

Log<sub>2</sub>-transformed RSEM TPM values (tumor, adjacent normal, and GTEx normal tissue) were downloaded from the TCGA Target GTEx study using the UCSC Xena platform. TCGA TARGET GTEx cohort was used. GTEx data was included to investigate whether histologically normal tissue adjacent to tumors had different expression levels, as previously indicated (Aran et al. 2017). Clinical data were obtained using the R package TCGAbiolinks and GDC Data Portal. For patients whose breast cancer subtypes were not

reported in the GDC legacy clinical data, additional subtype information was obtained from cBioPortal using the other TCGA legacy datasets.

## Relapse free survival

Disease-free months and relapse events were downloaded from cBioPortal (TCGA BRCA GDC Legacy). Patients were stratified into high and low *MDM2* expression groups using the “auto select best cutoff” feature of the KMplotter (Györfy 2021) where clinical and expression data were uploaded. Log<sub>2</sub>-transformed RSEM TPM values were downloaded from the TCGA Target GTEx study using the UCSC Xena platform. Patients with relapse-free survival times of 0 months or greater than 120 months (10 years) were excluded from the analysis.

## Results

### 3'UTR editing in breast cancers

Using the RNA editing sites defined in TCGA Breast Cancer RNA-seq dataset (TCGA-RNAediting, SynID: syn2374375) (Han et al. 2015), we detected differentially edited mRNAs in breast tumors (Fig. 1). Given that majority of differentially edited regions mapped to 3'UTRs, we focused on these editing events detected in all breast cancer subtypes (Table S1, Fig.S1a).

We started by experimentally confirming the A-to-I editing events in the 3'UTRs of selected transcripts based on their cancer relevance and high expression in breast tumors (Fig. S1b). Inosine (I) in the RNA is recognized as guanosine (G) by reverse transcriptase (RT), and therefore cytosine (C) is incorporated into the reverse-transcribed cDNA. Next, upon PCR amplification of the cDNA, DNA polymerase incorporates G into the new strand. Consequently,

A-to-I editing is observed as a complete or partial replacement of edited A with G in the cDNA (Malik et al. 2021).

To this end, we used primers (Table S2) flanking the editing sites and generated PCR amplicons by using genomic DNA or cDNA as templates. Following amplicon sequencing, we confirmed A-to-I(G) changes in the 3'UTRs of *MDM2* (mouse double minute 2 homolog), *GINS1* (GINS complex subunit 1), and *FIIR* (junctional adhesion molecule A) (Fig. 2a, b, c, Table S3). A-to-I(G) editing sites were quantified by calculating G count percentage in RNA-seq reads at positions where an A was present in the gDNA templated amplicons (Malik et al. 2021). The initial editing predictions for *MDM2*, *GINS1*, and *FIIR*, obtained from the TCGA breast cancer patient dataset was experimentally validated (Fig. 2). A few additional A-to-I(G) editing events were identified for *MDM2* that were not initially predicted (Fig. 2a, indicated by \*). Importantly, none of these edit sites were reported as SNPs based on the DBSNP (The Single Nucleotide Polymorphism Database). We also checked the Database of RNA Editing in Humans (DARNED), further confirming that these sites were edited in diverse tissues (Table S4-6). Among the editing sites we confirmed, chr12:69237004, chr12:69237010, chr12:69237013, and chr12:69237053 have been previously shown to be edited in breast cancer, 12 of 15 sites for *MDM2*, 8 of 9 sites for *GINS1*, 4 of 5 sites for *FIIR* of editing sites were also confirmed in lymphoblastoid cells according to DARNED (Bahn et al. 2012; Ramaswami et al. 2012). Moreover, independently amplified and sequenced PCR amplicons yielded comparable editing percentages in MCF7 cells, supporting the reproducibility of the results (Fig. S2a). Editing was further confirmed in MDA-MB-231 cells representing triple negative breast cancer cells (Fig. S2b-d).

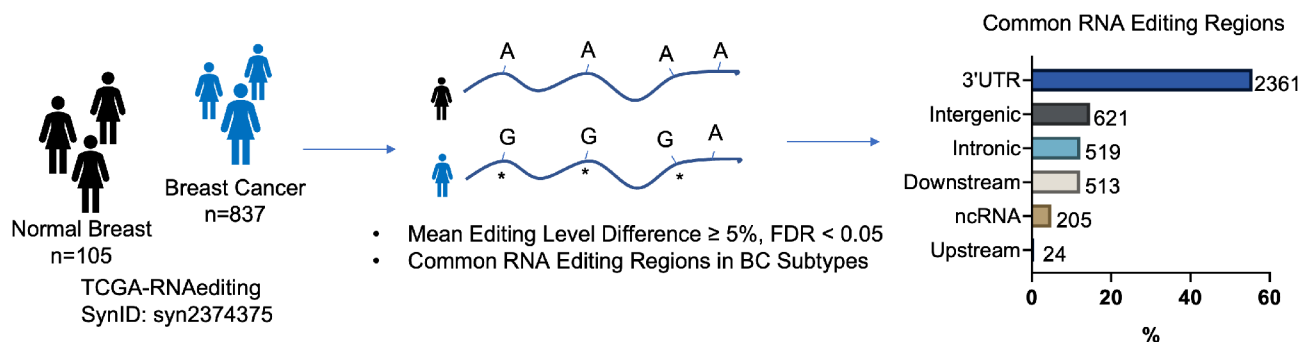


**Fig. 1** TCGA breast cancer ( $n=837$ ) and normal breast tissue ( $n=105$ ) RNA-seq data was screened for A-to-I(G) editing events. Informative RNA editing sites were identified in at least five tumor and non-tumor sample pairs. Differential editing was assessed using the Wilcoxon test, with significant sites defined by  $FDR < 0.05$  and a mean editing

level difference  $\geq 5\%$  between tumor and non-tumor samples. Majority of significant editing sites map to 3'UTRs. The upstream and downstream regions were defined as 1 kilobase (kb) sequences flanking the annotated transcription start and end sites of the gene, respectively. ncRNA: Noncoding RNA

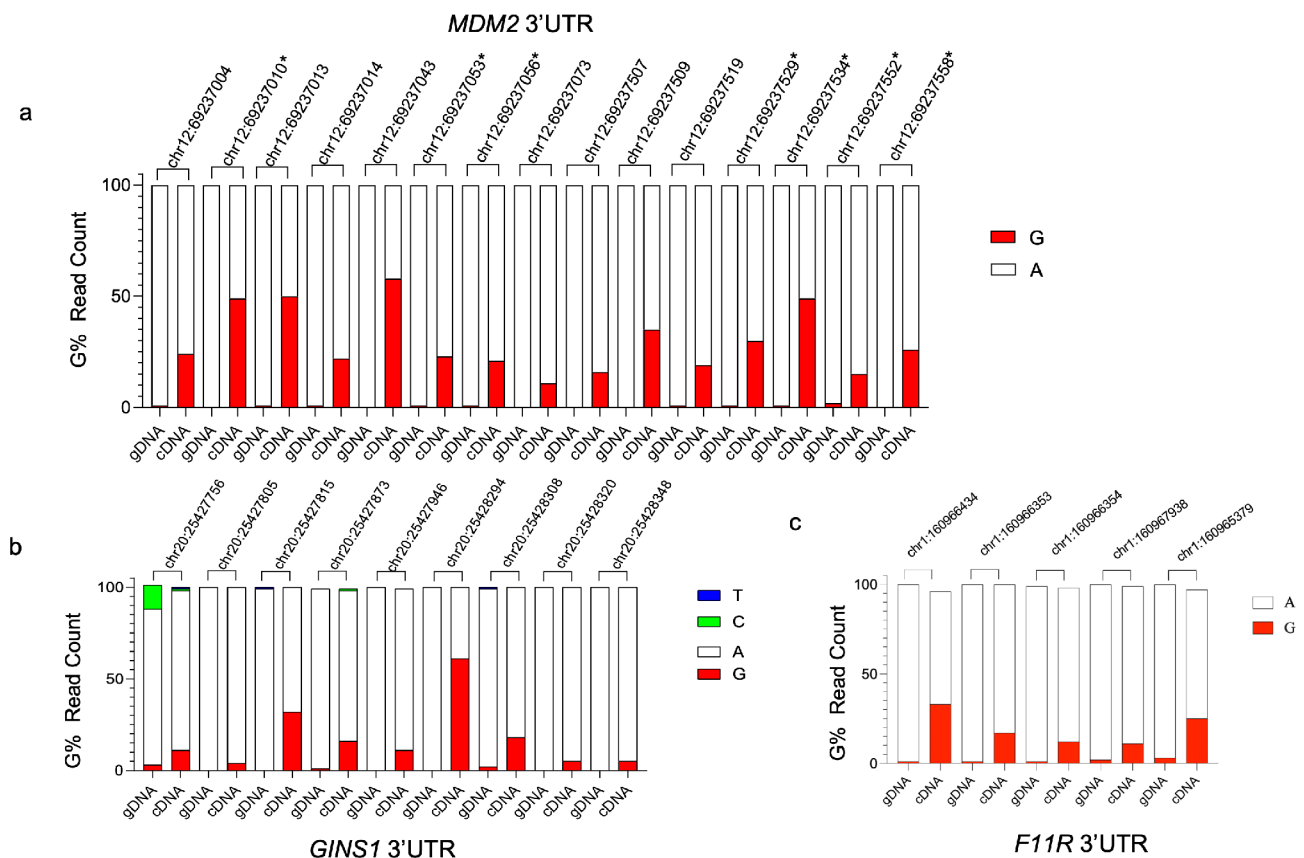


**Fig. 2** A-to-I(G) editing events in the 3'UTRs of *MDM2* (a), *GINS1* (b), and *F11R* (c) in MCF7 cells. gDNA (genomic DNA) or cDNA templated PCR amplicons were sequenced and G% values were calcu-

lated based on NGS read counts. The NGS confirmed A-to-I(G) editing events that were not initially predicted are indicated by \*

### ADAR1 interaction with the 3'UTRs of *MDM2*, *GINS1* and *F11R*

Next, to functionally test the relationship between ADAR1 and edited mRNAs, we performed ADAR1 immunoprecipitation of interacting RNAs and RT-PCR (RIP-PCR) to determine whether ADAR1 interacts with *MDM2*, *GINS1*, and *F11R* mRNAs. cDNAs were synthesized from ADAR1 immunoprecipitated RNAs using oligo (dT) or gene-specific primers. Editing events were examined in the MCF7 breast cancer model, representing the most common type of breast cancer (luminal A subtype), expressing estrogen receptor (ER) and/or progesterone receptor (PR) (Perou et al. 2000; Sorlie et al. 2003). Our results demonstrated that all three mRNAs, *MDM2*, *GINS1*, and *F11R* were specifically enriched in ADAR1 immunoprecipitation samples. In contrast, these mRNAs were not detected in the control samples immunoprecipitated with non-specific control IgG antibody (Fig. 3).

We also sought to investigate whether these interactions were functional and knocked down ADAR1 using RNAi and sequenced RT-PCR amplicons covering the previously edited regions for *MDM2*, *GINS1*, and *F11R*. All

three mRNAs, *MDM2*, *GINS1*, and *F11R* had markedly decreased editing levels compared to ADAR1-expressing cells. *MDM2* editing levels were similar in NT siRNA transfected cells and untransfected MCF7 cells (Fig. 4, Fig. S2e).

To this end, based on in silico editing predictions from tumors, we were able to experimentally confirm editing events in the 3'UTRs of selected candidates, showing their physical and functional relationship with ADAR1. Next, given its established role in cancer, we focused on RNA editing events in the 3'UTR of *MDM2*.

### *MDM2* overexpression and editing in breast cancer

First, we determined *MDM2* levels in breast cancers using GTEx normal breast tissue ( $n=179$ ), TCGA normal breast tissue ( $n=113$ ), and TCGA breast cancer tumor subtypes (luminal A ( $n=562$ ), luminal B ( $n=214$ ), basal ( $n=190$ ), HER2-enriched ( $n=81$ ), and normal-like ( $n=39$ )). Curiously, *MDM2* is most significantly overexpressed in luminal A (lumA) breast cancers in the TCGA dataset compared with normal breast tissue or adjacent normal tissue (Fig. 5a, b). For lumA tumors, high *MDM2* transcript levels correlate with poor relapse-free survival times ( $p<0.05$ ) (Fig. 5c). In

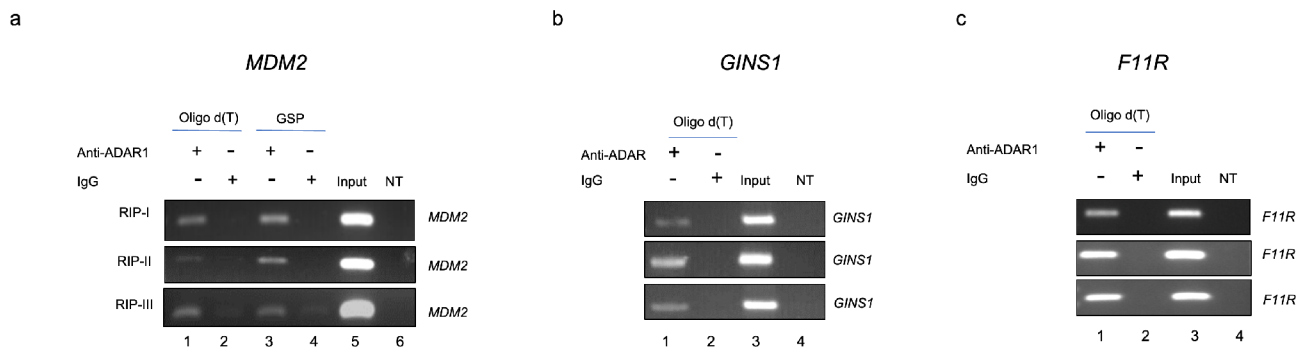


**Fig. 3** RIP-PCR for *MDM2* (a), *GINS1* (b) and *F11R* (c). For RNA-IP, ADAR1 (Abcam, ab168809), and rabbit IgG (Cell Signaling, 2729) antibodies were used. cDNAs were synthesized from RNA samples isolated after RIP with oligo d(T) primers (lanes 1, 2), or gene-specific primers (GSP) for *MDM2* (lanes 3,4). Three independent biological

replicates are shown for each RIP experiment and PCR. Lane 5 for *MDM2*, and lanes 3 for *GINS1* and *F11R* RIP-PCRs had MCF7 cDNA (Input) as positive control for PCR. NT lane was no template/negative control

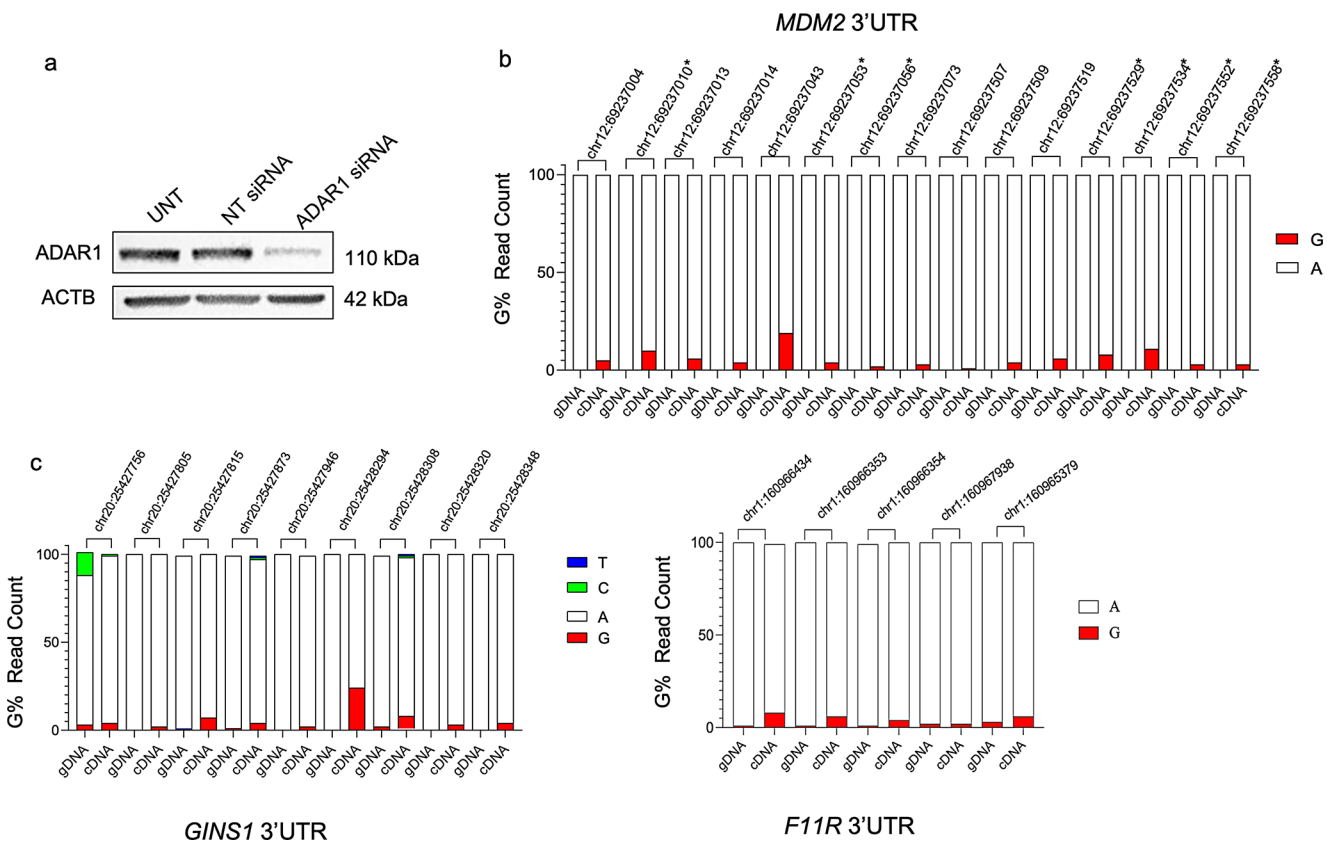


**Fig. 4** siRNA-mediated ADAR1 knockdown and RNA editing in MCF7 cells. a. Western blot shows ADAR1 protein levels in ADAR1 siRNA or NT (non-targeting) siRNA transfected cells. UNT: Untransfected cells. The same blots were hybridized with ACTB antibody to

test sample loading. b. A-to-I(G) editing ratios of *MDM2*. c. A-to-I(G) editing ratios of *GINS1*, and A-to-I(G) editing ratios of *F11R* in ADAR1 knockdown MCF7 cells

line with these findings, an earlier study suggested *MDM2* as an independent negative prognostic marker for breast cancer based on IHC performed in more than 2000 breast carcinomas (Turbin et al. 2006).

*MDM2* has an unusually long 3'UTR, harboring previously described cis-elements recognized by trans-factors, including microRNAs (Zhang et al. 2016). To investigate the

functional impact of RNA editing, we focused on the highly edited region within the *MDM2* 3'UTR. Double-stranded oligonucleotides were synthesized to mimic either the non-edited or edited state, where the edited oligo featured guanine (G) substitutions at the adenosine (A) positions for seven nucleotides within the highly edit-rich region of the *MDM2* 3'UTR. The edited and non-edited sequences were



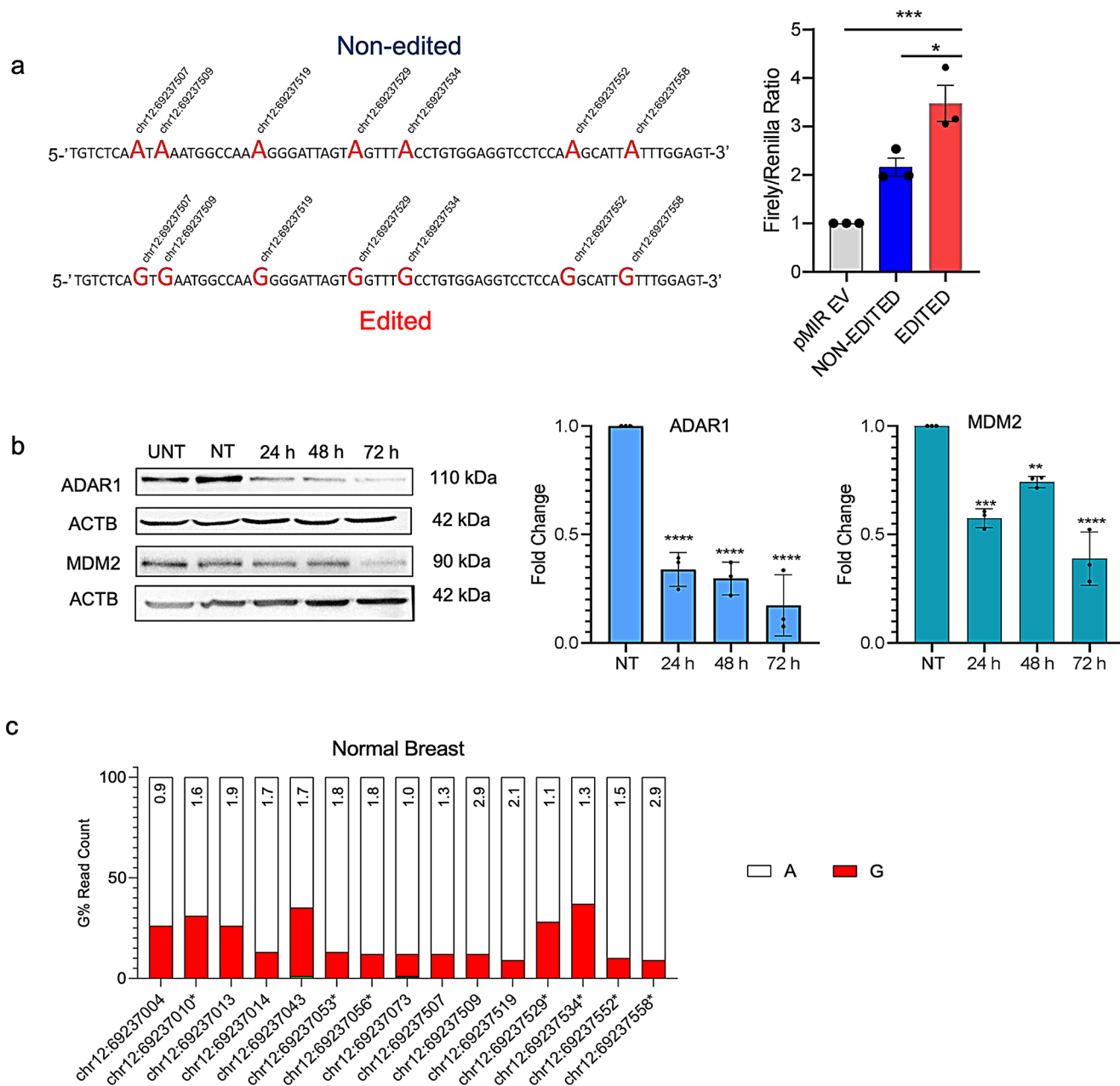


**Fig. 6** Effect of RNA editing on MDM2 protein levels, **(a)** Dual luciferase reporter assay with *MDM2* 3'UTR edit rich region. Non-edited (A) and edited (G) oligos were cloned downstream of the luciferase gene in pMIR. MCF7 cells were transiently transfected, and *Firefly/Renilla* luciferase read-outs from the constructs were normalized to that of empty pMIR (EV) ( $p < 0.05$ ,  $***p < 0.0005$ ,  $n = 3$  independent transfections, one-way ANOVA, Tukey's HSD), **(b)** ADAR1 and MDM2 protein levels in ADAR1 siRNA transfected (24 h, 48 h, 72 h) MCF7 cells. The same blots were hybridized with ACTB antibody

to test sample loading. The image is representative of 3 independent experiments. Graphs show densitometric quantification of MDM2 and ADAR1 bands normalized to NT siRNA transfected cells ( $**p < 0.005$ ,  $***p < 0.0005$ ,  $****p < 0.0001$ , one-way ANOVA, Tukey's HSD). NT: non-targeting siRNA transfected cells, UNT: Untransfected cells, **(c)** NGS and G% reads for the fifteen RNA editing positions for the 3'UTR of *MDM2* in normal breast tissue. Fold changes in RNA editing percentage values between MCF7 cells and normal breast cDNA are shown on the bars

kinetics compared to the original BirA biotin ligase (Roux et al. 2012). We transfected estrogen receptor-positive MCF7 cells with the CSTF2-TurboID construct and treated them with E2 (Estradiol) to stimulate transcription and proliferation (Ayaz et al. 2019). We confirmed the expression

and biotinylation potential of CSTF2-TurboID by incubating the cells with 50  $\mu$ M biotin for 3 h (Fig. 7a). Endogenous CSTF2 was mostly present in the nuclear fraction (n), whereas CSTF2-TurboID fusion protein was detected in both the nucleus and cytosol (c) (Fig. 7a). Of note, E2

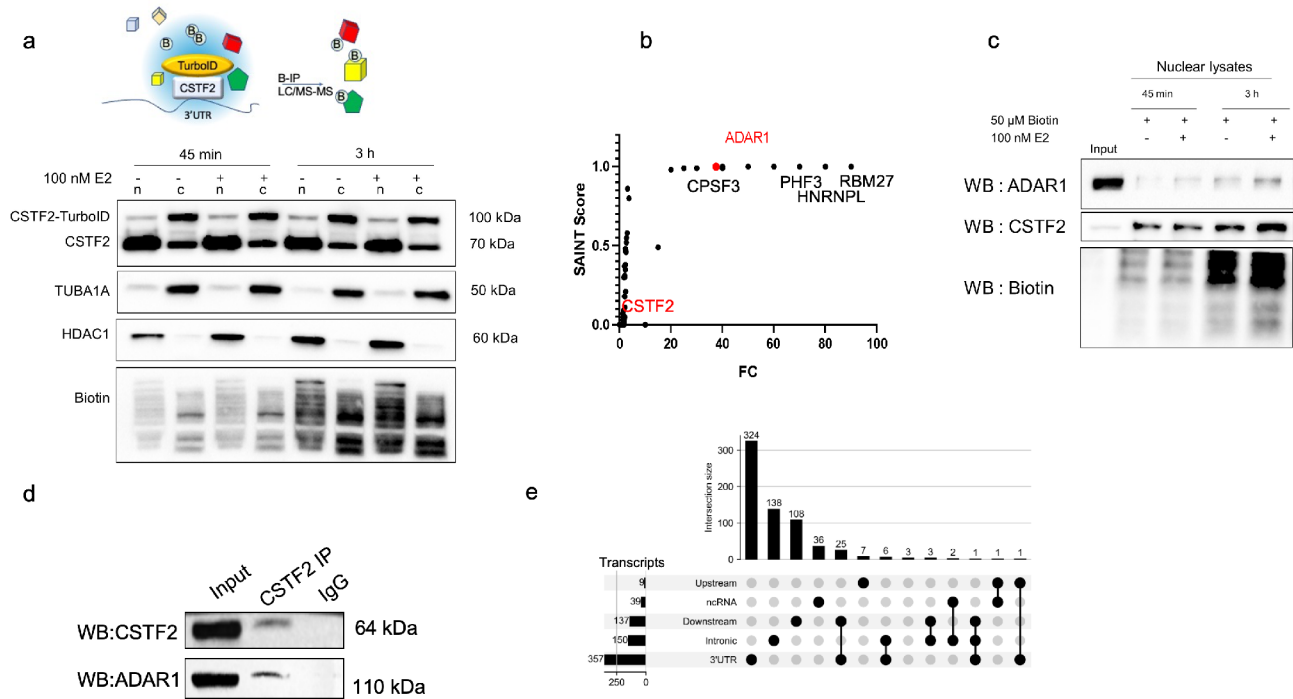


**Fig. 7** ADAR1 interacts with CSTF2, **a**. Schematic shows the proximity biotinylation approach to detect protein interactions at 3'UTRs using CSTF2 TurboID HA fusion protein expression and biotinylation in MCF7 cells. Biotinylated target proteins were immunoprecipitated (B-IP) and analyzed by LC-MS/MS. Western blot analysis of CSTF2-TurboID transfected MCF7 cells treated with 100 nM E2 or ethanol for 45 min–3 h, and 50 μM biotin. Nuclear and cytoplasmic lysates were subjected to western blot analysis using anti-CSTF2 antibody to detect CSTF2\_TurboID\_HA fusion and endogenous CSTF2. HDAC1 and TUBA1A antibodies were used to validate the nuclear and cytoplasmic fractions. Anti-Biotin antibody was used for biotinylation assessment, **b**. Biotinylated nuclear proteins were identified through LC-MS/MS analysis. ADAR1 was found to be significantly enriched among the biotinylation nuclear proteins (SAINT score 1), FC:40, BFD:0) (Fig. 7b, Table S8). Consistent with this interaction, ADAR1 is predominantly localized in the nucleus (Fig. S4).

fusion. MCF7 cells were transfected with CSTF2-TurboID. After 24 h, cells were incubated with 50 μM Biotin in the presence or absence of E2 for 45 min and 3 h. Isolated nuclear and cytoplasmic lysates were used for affinity capture with streptavidin beads. Eluted proteins were used for western blot analysis with anti-ADAR1, anti-CSTF2 and anti-Biotin antibodies, **d**. Nuclear extracts (500 μg) of MCF7 cells were subjected to Co-IP with CSTF2 or isotype-matched IgG. Input was 25 μg nuclear lysate. Immunoprecipitated proteins were then subjected to immunoblotting using CSTF2 or ADAR1 antibodies. WB: western blotting, **e**. Upset plot showing intersection of RNA editing events on mRNAs. Majority of RNA editing events were only detected on 3'UTRs. Each row represents a genomic feature, and the filled dots indicate the intersection of editing regions in individual mRNAs. The vertical bars indicate the number of genes in each category

treatment to enhance transcription and proliferation did not alter the subcellular localization of the fusion protein. Following this characterization, target proteins were labeled using the described conditions.

To capture nuclear targets of CSTF2-TurboID, biotinylation proteins in the nuclear and cytoplasmic lysates were separately captured using streptavidin-conjugated magnetic beads and subjected to LC-MS/MS analysis. The experiment was repeated twice, with two technical replicates for each sample (E2 or ethanol-treated). All biotinylation proteins in the cytoplasmic fraction were subtracted from the nuclear fraction and the SAINT algorithm was used to probabilistically score protein-protein interactions in E2 treated cells (Choi et al. 2011) (Fig. 7b). Of note, we did not capture any E2-specific biotinylation of proteins by the CSTF2-TurboID construct. In addition to the expected interactors of CSTF2 that appeared as biotinylation proteins (e.g., CSTF2 itself,

CPSF3, and CPSF2), 13 proteins had a SAINT score of 1. These candidates were considered high-confidence CSTF2 interactors (Table S8). Interestingly, ADAR1 emerged as one of the most significant nuclear interactors of CSTF2 (Saint Score 1, FC:40, BFD:0) (Fig. 7b, Table S8). Consistent with this interaction, ADAR1 is predominantly localized in the nucleus (Fig. S4).

To confirm the LC-MS/MS results and explore a potential interaction between ADAR1 and CSTF2, we first performed an independent proximity biotinylation experiment. CSTF2-TurboID biotinylation proteins were pulled down and subjected to western blotting. CSTF2 and ADAR1 were both found in the biotinylation fraction (Fig. 7c). Using an independent approach, we performed Co-IP in untransfected MCF7 cells. Immunoprecipitation of nuclear extracts using the CSTF2 antibody followed by immunoblotting with the ADAR1 antibody confirmed the presence of ADAR1 in the

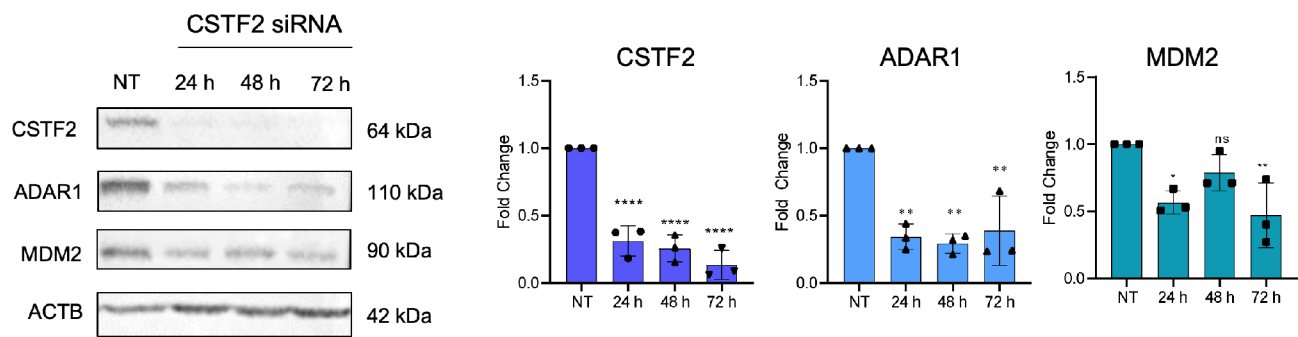


**Fig. 8** Effect of CSTF2 knockdown on ADAR1 and MDM2 protein levels. Western blot analysis of CSTF2 siRNA transfected MCF7 cells (24, 48, and 72 h) showed decreased ADAR1 and MDM2 protein levels. The same blots were hybridized with ACTB antibody to test sample loading. The image is representative of 3 independent experi-

ments. Graphs show densitometric quantification of bands normalized to NT bands (ns: not significant, \* $p < 0.05$ , \*\* $p < 0.01$ , \*\*\*\* $p < 0.0001$ ;  $n = 3$  biological replicates, one-way ANOVA, Tukey's HSD). NT: non-targeting siRNA transfected cells

immunoprecipitated lysates (Fig. 7d, Fig. S5 for biological replicates for the Co-IP experiment). These results suggest that ADAR1 interacts with CSTF2, a critical component of the polyadenylation machinery. In addition, we found that the majority of differentially edited mRNAs exhibited editing exclusively within their 3'UTRs, with no detectable editing in other transcript regions (Fig. 7e). This pattern may indicate a 3'UTR-specific accessibility or the selective recruitment of ADAR1 to these regions.

It remains unclear whether the interaction between ADAR1 and CSTF2 and/or other polyadenylation machinery components is essential for RNA editing at specific 3'UTRs, including *MDM2*. It is also not clear whether this interaction is direct and/or is RNA dependent. Possibly due to the essential role of CSTF2 in mRNA maturation, CSTF2 knockdown resulted in a 60% reduction in ADAR1, and 40–50% reduction in MDM2 protein levels, which precluded the ability to assess the role of the CSTF2-ADAR1 interaction in RNA editing under these conditions for *MDM2* (Fig. 8). Of note, siRNA-mediated knockdown of CSTF2 or ADAR1 in MCF7 cells did not result in a noticeable reduction of *MDM2* transcript levels and there was no correlation between *ADAR1* and *MDM2* mRNAs levels in the TCGA breast cancer RNA-seq data for LumA patients (Fig. S7). There is also no correlation between MDM2 and ADAR1 mRNA expression in Luminal A breast cancer samples (TCGA) (Fig. S7).

Overall, these findings highlight the impact of 3'UTRs and RNA editing on protein levels of MDM2 and potentially other cancer-related genes. Elucidating the mechanism of RNA editing for activation or inactivation of cancer-related genes may open new avenues for epitranscriptome targeted therapies in cancer.

## Discussion

Mutations and epitranscriptomic changes in coding regions may alter amino acid sequences and impact protein levels or activity in cancer cells. However, understanding the complex molecular mechanisms of cancers also requires investigating non-coding regions of mRNAs, such as 3'UTRs, which are crucial for regulating mRNA stability, localization, and translation efficiency (Erson-Bensan 2020). Supporting this, advances in sequencing technologies and computational analysis have revealed that variations in 3'UTR length and RNA modifications within 3'UTRs can significantly impact protein levels, not only in cancer but also in other diseases (Mitschka and Mayr 2022; Liu et al. 2024; Tac et al. 2021; Pinto and Levanon 2019).

Here we used in silico predictions from breast cancer patient RNA-seq data (Han et al. 2015) and determined upregulated editing events commonly detected in breast cancer subtypes. This approach showed an enrichment of upregulated A-to-I editing events in 3'UTRs. Of note, this enrichment is for the commonly edited mRNAs in all breast cancer subtypes, excluding subtype specific events. Additional editing events likely occur in a subtype specific manner and in other regions of mRNAs, as well as in spliced-out introns; however, such events typically go undetected in standard RNA-seq datasets unless the introns are exonized. Furthermore, alternative polyadenylation can generate transcript isoforms with variable 3'UTR lengths. In these cases, editing events that occur in extended 3'UTRs may be misannotated as intergenic regions when compared to canonical gene and isoform structures. As a result, sequencing strategies specifically tailored to capture all A-to-I editing events (Wei et al. 2023), coupled with isoform specific analyses are necessary for a more comprehensive characterization of the editing landscape.

We experimentally validated RNA editing sites in the 3'UTRs of *MDM2*, *GINS1*, and *FIIR*. Direct sequencing

of RT-PCR products allowed a quantitative comparison of nucleotide counts of cDNA and genomic DNA templated amplicons (Malik et al. 2021). Additional protein-based experiments showed the physical and functional interaction between the selected 3'UTRs and ADAR1.

Of these 3'UTRs, we focused on MDM2 given its role in cancer. MDM2 is best characterized for its E3 ligase activity and its role in the negative regulation of the major tumor suppressor TP53 (reviewed in Yousuf et al., 2025). MDM2 also regulates TP53-independent processes, including cell migration and metastasis (de Queiroz et al. 2024), and targets other proteins such as the microtubule-associated hematopoietic PBX-interaction protein (HPIP), a positive regulator of E2-mediated AKT signaling (Shostak et al. 2014). Although MDM2 gene amplification has been reported in luminal breast cancers (Wege et al. 2022), the role of epitranscriptomic mechanisms in MDM2 regulation remains largely unexplored in breast cancers. Additionally, correlation of high ADAR protein levels with poor relapse free survival in ER (+) breast tumors warrant further investigation (Fig. S6).

In this study, we identified and confirmed 15 distinct A-to-I(G) editing sites within the *MDM2* 3'UTR and showed seven editing sites to have a positive effect on protein levels in a reporter system. Silencing ADAR1 led to a reduction in A-to-I(G) editing across these 15 sites, accompanied by a significant decrease in MDM2 protein levels, underscoring the regulatory impact of RNA editing on MDM2 expression. Moreover, RNA editing ratios were less in normal breast tissue, suggesting a cancer-specific increase in RNA editing. A reporter assay provided initial insights into the functional potential of several *MDM2* RNA editing sites; however, a more comprehensive analysis using full-length constructs, combined with functional assays, would be more informative in determining whether microRNAs and/or other transacting factors differentially bind to the edited transcripts. Based on these results, we suggest, 3'UTR editing to be a contributor to increased MDM2 expression in breast cancers and propose that MDM2 protein can be significantly down-regulated by ADAR1 inhibition. Of note, ADAR1 inhibition in cancers may have additional advantages because some tumors depend on ADAR1 and A-to-I(G) editing to escape immune surveillance, potentially enabling anticancer therapies with ADAR1 inhibitors (Rehwinkel and Mehdipour 2025).

In addition, most editing sites are within dsRNA regions derived from the transcription of inverted-repeat *Alu* elements (Liu et al. 2024), but *MDM2* 3'UTR editing sites were not surrounded by *Alu* repeats, suggesting the involvement of other sequences and/or other RNA-binding proteins. Proximity biotinylation by CSTF2 TurboID, LC-MS/MS and co-immunoprecipitation results demonstrated the interaction of

ADAR1 and CSTF2, a key polyadenylation machinery protein, opening the possibility to better understand ADAR1 presence in 3'UTRs. The interaction between ADAR1 and CSTF2 may have further implications as was suggested in glioblastoma cells (Bahn et al. 2015). In U87MG cells, ADAR1 has been shown to compete with known 3'UTR-binding factors, highlighting how its occupancy—and that of polyadenylation proteins or other RBPs—can be shaped by tissue-specific regulatory contexts.

In closing this study highlights the significance of A-to-I(G) RNA editing in the 3'UTR of *MDM2* and its contribution to increased MDM2 expression in breast cancers. Our findings demonstrate that RNA editing positively influences MDM2 protein levels, with seven specific editing sites enhancing protein expression in a reporter system. The cancer-specific elevation of RNA editing and the reduction of MDM2 levels upon ADAR1 silencing underscore the regulatory role of ADAR1-mediated 3'UTR editing. Additionally, the interaction between ADAR1 and CSTF2 suggests a complex interplay between RNA editing and mRNA processing. Future studies exploring the functional implications of ADAR1-CSTF2 interaction will also be essential for unraveling the complex dynamics and consequences of RNA editing in cancer progression and treatment strategies.

**Supplementary Information** The online version contains supplementary material available at <https://doi.org/10.1007/s10142-025-01611-3>.

**Acknowledgements** We thank Ali Yurtseven for his help in SAINT analysis.

**Author contributions** EA and DK performed experiments, MC performed TurboID experiments, DND performed bioinformatic analysis for MDM2, HAT performed in silico RNA editing predictions, OUS supervised editing predictions, EC verified TurboID experiments. IG contributed to the Co-IP experiments, BAA and NO contributed to the proteomic studies, AEEB conceptualized the work; and drafted and reviewed the manuscript. All authors contributed to the writing of the manuscript.

**Funding** Open access funding provided by the Scientific and Technological Research Council of Türkiye (TÜBİTAK). This project was funded by the TÜBİTAK 122Z329 and 118Z745. EA was supported by TÜBİTAK BİDEB 2210 A.

**Data availability** Data is provided within the manuscript or supplementary information files.

## Declarations

**Ethics approval and consent to participate** Not applicable.

**Consent for publication** Not applicable.

**Competing interests** The authors declare no competing interests.

**Open Access** This article is licensed under a Creative Commons Attribution 4.0 International License, which permits use, sharing, adaptation, distribution and reproduction in any medium or format, as long as you give appropriate credit to the original author(s) and the source, provide a link to the Creative Commons licence, and indicate if changes were made. The images or other third party material in this article are included in the article's Creative Commons licence, unless indicated otherwise in a credit line to the material. If material is not included in the article's Creative Commons licence and your intended use is not permitted by statutory regulation or exceeds the permitted use, you will need to obtain permission directly from the copyright holder. To view a copy of this licence, visit <http://creativecommons.org/licenses/by/4.0/>.

## References

- Aran D, Camarda R, Odegaard J, Paik H, Oskotsky B, Krings G, Goga A, Sirota M, Butte AJ (2017) Comprehensive analysis of normal adjacent to tumor transcriptomes. *Nat Commun* 8(1):1077. <https://doi.org/10.1038/s41467-017-01027-z> PMID: 29057876; PMCID: PMC5651823
- Ayaz G, Yasar P, Olgun CE, Karakaya B, Kars G, Razizadeh N, Yavuz K, Turan G, Muyan M (2019) Dynamic transcriptional events mediated by estrogen receptor alpha. *Front Biosci (Landmark Ed)*;24(2):245–276. <https://doi.org/10.2741/4716>. PMID: 30468654
- Bahn JH, Lee JH, Li G, Greer C, Peng G, Xiao X (2012) Accurate identification of A-to-I RNA editing in human by transcriptome sequencing. *Genome Res* 22(1):142–150. <https://doi.org/10.1101/gr.124107.111> Epub 2011 Sep 29. PMID: 21960545; PMCID: PMC3246201
- Bahn JH, Ahn J, Lin X, Zhang Q, Lee JH, Civelek M, Xiao X (2015) Genomic analysis of ADAR1 binding and its involvement in multiple RNA processing pathways. *Nat Commun* 6:6355. <https://doi.org/10.1038/ncomms7355> PMID: 25751603; PMCID: PMC4355961
- Bass BL (2002) RNA editing by adenosine deaminases that act on RNA. *Annu Rev Biochem* 71:817–846. <https://doi.org/10.1146/annurev.biochem.71.110601.135501> Epub 2001 Nov 9. PMID: 12045112; PMCID: PMC1823043
- Choi H, Larsen B, Lin ZY, Breikreutz A, Mellacheruvu D, Fermin D, Qin ZS, Tyers M, Gingras AC, Nesvizhskii AI (2011) SAINT: probabilistic scoring of affinity purification-mass spectrometry data. *Nat Methods* 8(1):70–73. <https://doi.org/10.1038/nmeth.1541> Epub 2010 Dec 5. PMID: 21131968; PMCID: PMC3064265
- de Queiroz RM, Efe G, Guzman A, Hashimoto N, Kawashima Y, Tanaka T, Rustgi AK, Prives C (2024) Mdm2 requires Sprouty4 to regulate focal adhesion formation and metastasis independent of p53. *Nat Commun* 15(1):7132. <https://doi.org/10.1038/s41467-024-51488-2> PMID: 39164253; PMCID: PMC11336179
- Erson-Bensan AE (2020) RNA-biology ruling cancer progression? Focus on 3'UTRs and splicing. *Cancer Metastasis Rev*;39(3):887–901. <https://doi.org/10.1007/s10555-020-09884-9>. PMID: 32361913
- Fumagalli D, Gacquer D, Rothé F, Lefort A, Libert F, Brown D, Khedoumi N, Shlien A, Konopka T, Salgado R, Larsimont D, Polyak K, Willard-Gallo K, Desmedt C, Piccart M, Abramowicz M, Campbell PJ, Sotiriou C, Detours V (2015) Principles governing A-to-I RNA editing in the breast Cancer transcriptome. *Cell Rep* 13(2):277–289 Epub 2015 Oct 1. PMID: 26440892; PMCID: PMC5326813
- Györfy B (2021) Survival analysis across the entire transcriptome identifies biomarkers with the highest prognostic power in breast cancer. *Comput Struct Biotechnol J* 19:4101–4109. <https://doi.org/10.1016/j.csbj.2021.07.014> PMID: 34527184; PMCID: PMC8339292
- Han L, Diao L, Yu S, Xu X, Li J, Zhang R, Yang Y, Werner HMJ, Eterovic AK, Yuan Y, Li J, Nair N, Minelli R, Tsang YH, Cheung LWT, Jeong KJ, Roszik J, Ju Z, Woodman SE, Lu Y, Scott KL, Li JB, Mills GB, Liang H (2015) The genomic landscape and clinical relevance of A-to-I RNA editing in human cancers. *Cancer Cell* 28(4):515–528 Epub 2015 Oct 1. PMID: 26439496; PMCID: PMC4605878
- Liu W, Wu Y, Zhang T, Sun X, Guo D, Yang Z (2024) The role of DsRNA A-to-I editing catalyzed by ADAR family enzymes in the pathogenesis. *RNA Biol* 21(1):52–69 Epub 2024 Oct 24. PMID: 39449182; PMCID: PMC11520539
- Maas S, Kawahara Y, Tamburro KM, Nishikura K (2006) Jan-Mar A-to-I RNA editing and human disease. 3(1):1–9. <https://doi.org/10.4161/ma.3.1.2495>. Epub 2006 Jan 12. PMID: 17114938; PMCID: PMC2947206 RNA Biol
- Malik TN, Cartiailler JP, Emeson RB (2021) Quantitative analysis of Adenosine-to-Inosine RNA editing. *Methods Mol Biol* 2181:97–111. [https://doi.org/10.1007/978-1-0716-0787-9\\_7](https://doi.org/10.1007/978-1-0716-0787-9_7) PMID: 32729077; PMCID: PMC8208106
- Mendoza HG, Beal PA (2024) Structural and functional effects of inosine modification in mRNA. *RNA* 30(5):512–520. <https://doi.org/10.1261/rna.079977.124> PMID: 38531652; PMCID: PMC11019749
- Mitschka S, Mayr C (2022) Context-specific regulation and function of mRNA alternative polyadenylation. *Nat Rev Mol Cell Biol* 23(12):779–796. <https://doi.org/10.1038/s41580-022-00507-5> Epub 2022 Jul 7. PMID: 35798852; PMCID: PMC9261900
- Peng X, Xu X, Wang Y, Hawke DH, Yu S, Han L, Zhou Z, Mojumdar K, Jeong KJ, Labrie M, Tsang YH, Zhang M, Lu Y, Hwu P, Scott KL, Liang H, Mills GB (2018) A-to-I RNA editing contributes to proteomic diversity in Cancer. *Cancer Cell* 33(5):817–828 Epub 2018 Apr 26. PMID: 29706454; PMCID: PMC5953833
- Peritz T, Zeng F, Kannanayakal TJ, Kilk K, Eiriksdóttir E, Langel U, Eberwine J (2006) Immunoprecipitation of mRNA-protein complexes. *Nat Protoc*;1(2):577–80. <https://doi.org/10.1038/nprot.2006.82>. PMID: 17406284
- Perou CM, Sørlie T, Eisen MB, van de Rijn M, Jeffrey SS, Rees CA, Pollack JR, Ross DT, Johnsen H, Akslen LA, Fluge O, Pergamenschikov A, Williams C, Zhu SX, Lønning PE, Børresen-Dale AL, Brown PO, Botstein D (2000) Molecular portraits of human breast tumours. *Nature*;406(6797):747–52. <https://doi.org/10.1038/3835021093>. PMID: 10963602
- Pinto Y, Levanon EY (2019) Computational approaches for detection and quantification of A-to-I RNA-editing. *Methods* 156:25–31. <https://doi.org/10.1016/j.ymeth.2018.11.011> Epub 2018 Nov 20. PMID: 30465820
- Ramaswami G, Lin W, Piskol R, Tan MH, Davis C, Li JB (2012) Accurate identification of human Alu and non-Alu RNA editing sites. *Nat Methods*;9(6):579–81. doi: 10.1038/nmeth.1982. Epub 2012 Apr 4. PMID: 22484847; PMCID: PMC3662811
- Rehwinkel J, Mehdiipour P (2025) ADAR1: from basic mechanisms to inhibitors. *Trends Cell Biol* 35(1):59–73. <https://doi.org/10.1016/j.tcb.2024.06.006> Epub 2024 Jul 18. PMID: 39030076; PMCID: PMC11718369
- Roux KJ, Kim DI, Raida M, Burke B (2012) A promiscuous biotin ligase fusion protein identifies proximal and interacting proteins in mammalian cells. *J Cell Biol* 196(6):801–810. <https://doi.org/10.1083/jcb.201112098> Epub 2012 Mar 12. PMID: 22412018; PMCID: PMC3308701
- Shostak K, Patrascu F, Göktuna SI, Close P, Borgs L, Nguyen L, Olivier F, Rammal A, Brinkhaus H, Bentires-Alj M, Marine JC, Chariot A (2014) MDM2 restrains estrogen-mediated AKT activation by promoting TBK1-dependent HPIP degradation. *Cell Death Differ*

- 21(5):811–824 Epub 2014 Jan 31. PMID: 24488098; PMCID: PMC3978309
- Sorlie T, Tibshirani R, Parker J, Hastie T, Marron JS, Nobel A, Deng S, Johnsen H, Pesich R, Geisler S, Demeter J, Perou CM, Lønning PE, Brown PO, Børresen-Dale AL, Botstein D (2003) Repeated observation of breast tumor subtypes in independent gene expression data sets. *Proc Natl Acad Sci U S A* 100(14):8418–8423. <https://doi.org/10.1073/pnas.0932692100>Epub 2003 Jun 26. PMID: 12829800; PMCID: PMC166244
- Tac HA, Koroglu M, Sezerman U (2021) RDDSV: accurate prediction of A-to-I RNA editing sites from sequence using support vector machines. *Funct Integr Genomics* 21(5–6):633–643. <https://doi.org/10.1007/s10142-021-00805-9>Epub 2021 Sep 16. PMID: 34529170
- Turbin DA, Cheang MC, Bajdik CD, Gelmon KA, Yorida E, De Luca A, Nielsen TO, Huntsman DG, Gilks CB (2006) MDM2 protein expression is a negative prognostic marker in breast carcinoma. *Mod Pathol*;19(1):69–74. <https://doi.org/10.1038/modpathol.3800484>. PMID: 16258514
- Wege AK, Rom-Jurek EM, Jank P, Denkert C, Ugoçsai P, Solbach C, Blohmer JU, Sinn B, van Mackelenbergh M, Möbus V, Trumpp A, Marangoni E, Pfarr N, Irlbeck C, Warfsmann J, Polzer B, Weber F, Ortman O, Loibl S, Vladimirova V, Brockhoff G (2022) *mdm2* gene amplification is associated with luminal breast cancer progression in humanized PDX mice and a worse outcome of Estrogen receptor positive disease. *Int J Cancer* 150(8):1357–1372. <https://doi.org/10.1002/ijc.33911>Epub 2021 Dec 28. PMID: 34927257
- Wei Q, Han S, Yuan K, He Z, Chen Y, Xi X, Han J, Yan S, Chen Y, Yuan B, Weng X, Zhou X (2023) Transcriptome-wide profiling of A-to-I RNA editing by Slic-seq. *Nucleic Acids Res* 51(16):e87. <https://doi.org/10.1093/nar/gkad604>PMID: 37470992; PMCID: PMC10484733
- Yousuf A, Khan NU (2025) Targeting MDM2-p53 interaction for breast cancer therapy. *Oncol Res* 33(4):851–861. <https://doi.org/10.32604/or.2025.058956>PMID: 40191734; PMCID: PMC11964874
- Zhang L, Yang CS, Varelas X, Monti S (2016) Altered RNA editing in 3' UTR perturbs microRNA-mediated regulation of oncogenes and tumor-suppressors. *Sci Rep* 6:23226. <https://doi.org/10.1038/srep23226>PMID: 26980570; PMCID: PMC4793219
- Zhang Y, Li L, Mendoza JJ, Wang D, Yan Q, Shi L, Gong Z, Zeng Z, Chen P, Xiong W (2024) Advances in A-to-I RNA editing in cancer. *Mol Cancer* 23(1):280. <https://doi.org/10.1186/s12943-024-02194-6>PMID: 39731127; PMCID: PMC11673720

**Publisher's note** Springer Nature remains neutral with regard to jurisdictional claims in published maps and institutional affiliations.